

# Comparative study on three highly sensitive absorption measurement techniques characterizing lithium niobate over its entire transparent spectral range

M. Leidinger,<sup>1,\*</sup> S. Fieberg,<sup>2</sup> N. Waasem,<sup>2</sup>  
F. Kühnemann,<sup>2</sup> K. Buse<sup>1,2</sup> and I. Breunig<sup>1</sup>

<sup>1</sup> University of Freiburg, IMTEK, Georges-Köhler-Allee 102, 79110 Freiburg, Germany

<sup>2</sup> Fraunhofer Institute for Physical Measurement Techniques, Heidenhofstraße 8,  
79110 Freiburg, Germany

[\\*markus.leidinger@uni-freiburg.de](mailto:markus.leidinger@uni-freiburg.de)

**Abstract:** We employ three highly sensitive spectrometers: a photoacoustic spectrometer, a photothermal common-path interferometer and a whispering-gallery-resonator-based absorption spectrometer, for a comparative study of measuring the absorption coefficient of nominally transparent undoped, congruently grown lithium niobate for ordinarily and extraordinarily polarized light in the wavelength range from 390 to 3800 nm. The absorption coefficient ranges from below  $10^{-4} \text{ cm}^{-1}$  up to  $2 \text{ cm}^{-1}$ . Furthermore, we measure the absorption at the Urbach tail as well as the multiphonon edge of the material by a standard grating spectrometer and a Fourier-transform infrared spectrometer, providing for the first time an absorption spectrum of the whole transparency window of lithium niobate. The absorption coefficients obtained by the three highly sensitive and independent methods show good agreement.

© 2015 Optical Society of America

**OCIS codes:** (300.1030) Absorption; (130.3730) Lithium niobate; (140.4780) Optical resonators; (300.6430) Spectroscopy, photothermal; (110.5125) Photoacoustics.

---

## References and links

1. ISO, "Optics and optical instruments—Lasers and laser-related equipment – Test method for absorbance of optical laser components," ISO 11551:2003.
2. A. Tam, "Applications of photoacoustic sensing techniques," *Rev. Mod. Phys.* **58**, 381–431 (1986).
3. N. Waasem, S. Fieberg, J. Hauser, G. Gomez, D. Haertle, F. Kühnemann and K. Buse, "Photoacoustic absorption spectrometer for highly transparent dielectrics with parts-per-million sensitivity," *Rev. Sci. Instrum.* **84**, 023109 (2013).
4. A. Alexandrovski, M. M. Fejer, A. Markosian and R. Route, "Photothermal common-path interferometry (PCI): new developments," *Proc. SPIE* **7193**, 71930D (2009).
5. A. Alexandrovski, Stanford Photo-Thermal Solutions 13-3547 Maile Street Pahoa, HI 96778 (private communication, 2013).
6. R. DeSalvo, A. Said, D. J. Hagan, E. W. Van Stryland and M. Sheik-Bahae, "Infrared to ultraviolet measurements of two-photon absorption and  $n_2$  in wide bandgap solids," *IEEE J. Quant. Electr.* **32**, 1324–1333 (1996).
7. M. Gunttau and W. Triebel, "Novel method to measure bulk absorption in optically transparent materials," *Rev. Sci. Instrum.* **71**, 2279–2282 (2000).

8. A. A. Savchenkov, V. S. Ilchenko, A. B. Matsko and L. Maleki, "Kilohertz optical resonances in dielectric crystal cavities," *Phys. Rev. A* **70**, 051804 (2004).
9. J. R. Schwesyg, M. C. C. Kajiyama, M. Falk, D. Jundt, K. Buse and M. M. Fejer, "Light absorption in undoped congruent and magnesium-doped lithium niobate crystals in the visible wavelength range," *Appl. Phys. B* **100**, 109–115 (2010).
10. J. R. Schwesyg, C. R. Phillips, K. Ioakeimidi, M. C. C. Kajiyama, M. Falk, D. H. Jundt, K. Buse and M. M. Fejer, "Suppression of mid-infrared light absorption in undoped congruent lithium niobate crystals," *Opt. Lett.* **35**, 1070–1072 (2010).
11. A. Gröne and S. Kapphan, "Higher vibrational states of OH/OD in the bulk of congruent LiNbO<sub>3</sub> and in proton/deuteron exchanged layers at the surface of LiNbO<sub>3</sub>," *J. Phys. Condens. Matter* **7**, 6393–6405 (1995).
12. A. Förster, S. Kapphan and M. Wöhlecke, "Overtone spectroscopy of the OH and OD stretch modes in LiNbO<sub>3</sub>," *Phys. Stat. Sol. B* **143**, 755–764 (1987).
13. M. L. Gorodetsky and V. S. Ilchenko, "Optical microsphere resonators: optimal coupling to high-Q whispering-gallery modes," *J. Opt. Soc. Am. B* **16**, 147 (1999).
14. A. B. Matsko, A. A. Savchenkov and L. Maleki, "Ring-down spectroscopy for studying properties of CW Raman lasers," *Opt. Commun.* **260**, 662–665 (2006).
15. P. A. Arsenev and B. A. Baranov, "Properties of the ions of the iron transition group in the lattice of single-crystalline lithium niobate," *phys. stat. sol. (a)* **9**, 673–677 (1972).
16. M. Vainio, J. Peltola, S. Persijn, F. J. M. Harren and L. Halonen, "Thermal effects in singly resonant continuous-wave optical parametric oscillators," *Appl. Phys. B* **94**, 411–427 (2009).
17. K. Buse, F. Jerman and E. Krätzig, "Two-step photorefractive hologram recording in LiNbO<sub>3</sub>:Fe," *Ferroelectrics* **141**, 197–205 (1993).
18. M. E. Lines, "Ultralow-loss glasses," *Annu. Rev. Mater. Sci.* **16**, 113–135 (1986).
19. A. A. Savchenkov, A. B. Matsko, V. S. Ilchenko and L. Maleki, "Optical resonators with ten million finesse," *Opt. Express* **15**, 6768–6773 (2007).

## 1. Introduction

With the availability of laser sources reaching nowadays several kW of light power the demands on optical materials increase. Optical elements have to be very transparent since even small absorption below  $10^{-2} \text{ cm}^{-1}$  can cause damage, because the absorbed power for a light beam of 1 kW is already 10 W for 1 cm sample thickness. Regarding laser sources, especially those based on optically nonlinear crystals require high power. The strong pump beam in combination with the crystal absorption leads to undesired effects as thermal lensing and detuning of the phase matching, limiting the performance of the light source. Thus, knowing the absorption of an optical material, especially in its highly transparent region, is the key to understand its limitations. The spectra may also provide hints for an improvement of their transparency, in particular if defects can be identified based on their spectral fingerprint.

The standard methods to measure absorption like grating spectroscopy (GS) or Fourier-transform infrared spectroscopy (FTIR) require an absorption of at least 1 % for a reasonable signal-to-noise-ratio (SNR). In a cm-sized sample, this leads to a measurable absorption coefficient of  $\geq 10^{-2} \text{ cm}^{-1}$ . To overcome this limitation, one can increase the sample thickness. In many cases, however, this is not possible. Thus, more sensitive methods are needed. Different techniques for measuring low absorption coefficients are nowadays available. Mostly, they exploit the fact that the majority of the absorbed energy is transferred into heat. Thus, laser calorimetry (LC) measures the increase in temperature directly and has become an ISO standard method [1]. Photoacoustic sensing (PAS) of small absorption is widely used for gases and liquids [2] and has recently been successfully applied to solid state materials as well [3]. Here, the pressure wave caused by pulsed illumination, local heating and thermal expansion of the sample can be measured using a microphone or a piezoelectric transducer. Furthermore, different thermal lensing techniques exist, that detect the change of the refractive index due to the increase in temperature, like photothermal common-path interferometry (PCI) [4] and the laser-induced deflection technique (LID) [7]. Both methods are based on a pump-probe technique with a high-power pump beam inducing the temperature change and a weak probe beam, which is disturbed by the inhomogeneous refractive index profile.

The development of whispering gallery resonators (WGR) has given rise to a new highly sensitive loss measurement method. In these monolithic cavities, light is guided by total internal reflection and is attenuated only by absorption and scattering of the bulk material. For highly transparent materials the light travels up to several km in the sphere, thereby overcoming the limitation of small optical path length for standard spectrometers. So far WGRs have been employed to determine the materials bulk attenuation for a few wavelengths only [8]. More detailed absorption spectra have not been taken by this method, yet.

Most highly sensitive techniques, like PAS, PCI or LID, are indirect and/or rely on a calibration. Thus, the material being characterized, has, e.g., to show a strong absorption band, that can be determined by standard methods, such as GS or FTIR and then be used for calibration. To evaluate the reliability of such a calibration and thus, of the measured values, the comparison of different techniques, measuring small absorption, is important. Despite a number of publications about different methods, there is still a lack of such a comparative study. Our aim is to compare the photoacoustic spectrometry (PAS), the photothermal common-path interferometry (PCI) and the whispering-gallery-resonator-based absorption spectrometry (WGRAS). Furthermore, we compare the obtained spectra at the points of higher absorption to those of the same sample studied with a grating spectrometer (GS) and a Fourier transform infrared spectrometer (FTIR).

As the sample for this study we have chosen an undoped, congruently grown lithium niobate crystal ( $\text{LiNbO}_3$ ). The material is important for nonlinear frequency conversion due to its high nonlinear-optical coefficients, the possibility to create quasi phase matching domain structures and its low absorption over a wide spectral range.

The sample preparation and its characteristics will be discussed in the following section 2. Subsequently, the three sections 3, 4 and 5 will describe PAS, PCI and WGRAS, respectively, their results and limitations. In chapter 6 the absorption spectra are compared also with data obtained by a GS, followed by a discussion of the advantages and disadvantages of the three methods applied (section 7) and a conclusion of the findings (chapter 8).

## 2. Sample preparation and characteristics

The transparency window of  $\text{LiNbO}_3$  is given by the band edge at around 320 nm and the multiphonon absorption in the IR, starting at around 3000 nm (see Fig. 1). As the absorption here is larger than  $10^{-2} \text{ cm}^{-1}$ , the edges can be resolved easily by standard methods, such as GS and FTIR. Published absorption spectra for undoped  $\text{LiNbO}_3$  also exist only for the edges of the transparency window [9, 10]. In the range from 800 to 2000 nm the absorption coefficient is still not known, as GS and FTIR reach their detection limit (see Fig. 1).

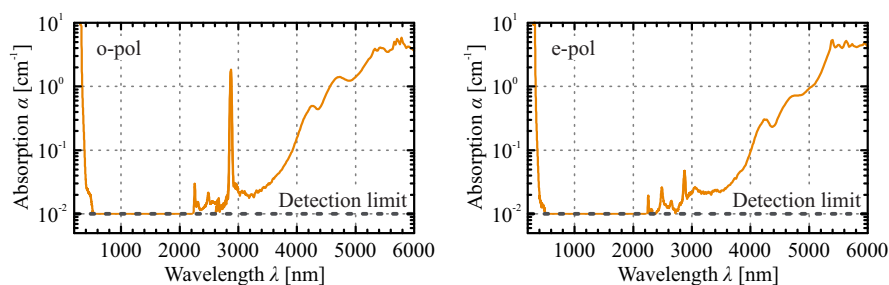


Fig. 1. Absorption spectra of undoped, congruently grown  $\text{LiNbO}_3$  for ordinarily (left) and extraordinarily (right) polarized light, measured with a grating spectrometer (GS, 200 to 3000 nm) and a Fourier transform infrared spectrometer (FTIR, 3000 to 6000 nm).

The absorption coefficients of  $\text{LiNbO}_3$  may vary, depending on the position in the grown boule and on the manufacturer. In order to compare different spectrometer types, it is hence crucial to employ the same sample for all measurements, as it is done in this work. As a preparation for the measurements, the crystal has been cut into two pieces, the first with the dimensions of  $11.7 \times 6.8 \times 6.1 \text{ mm}^3$  ( $z, x, y$ ) for PAS, PCI, GS and FTIR measurements and the second piece was used to manufacture a whispering gallery resonator of 0.5 mm height ( $z$ ) and a diameter of about 2 mm ( $x, y$ ).

### 3. Photoacoustic spectroscopy (PAS)

#### 3.1. Measurement principle

This section gives a short description of photoacoustic spectroscopy (PAS, [2]) employed for the measurements presented in this article. A detailed description can be found in [3]. The measurement principle is shown in Fig. 2. A focused nanosecond laser pulse illuminates the sample and, due to absorption, deposits some part of its energy inside the material. This leads to local heating after thermalization of the deposited energy. As a consequence, thermal expansion causes the emission of a pressure wave. A piezoelectric transducer attached to the edge of the sample detects the photoacoustic wave.

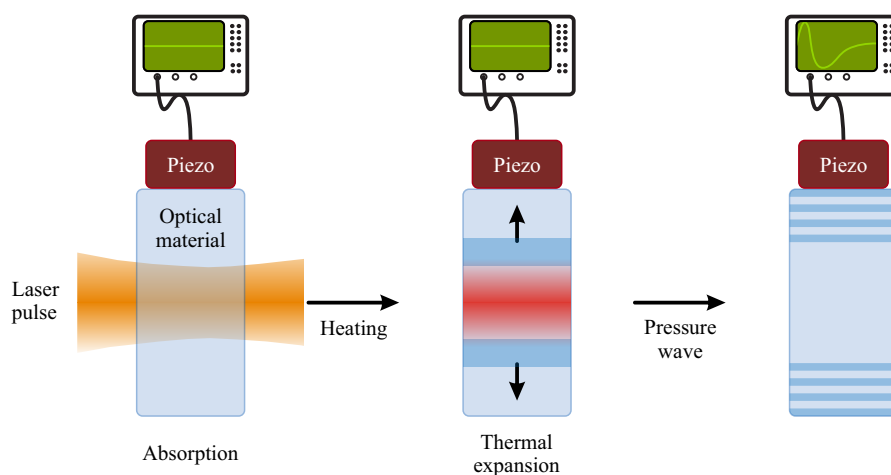


Fig. 2. Measurement principle of the photoacoustic spectrometer: Partial absorption of a laser pulse leads to a heating of the sample, which causes a pressure wave due to thermal expansion. This acoustic wave then travels through the crystals and is detected by a piezoelectric transducer, attached to the surface of the sample.

The voltage  $U_{\text{PhAc}}$  at the detector, corresponding to the peak pressure of the acoustic wave, is proportional to the amount of absorbed light energy. Knowing the incident pulse energy  $E_{\text{pulse}}$  and a wavelength independent calibration coefficient  $K$ , one can determine the absorption coefficient  $\alpha$ :

$$\alpha = \frac{U_{\text{PhAc}}}{E_{\text{pulse}}K} = \frac{S_{\text{PhAc}}}{K}, \quad (1)$$

with the photoacoustic signal  $S_{\text{PhAc}} = U_{\text{PhAc}}/E_{\text{pulse}}$ .

In the presented setup a nanosecond laser system is used as the pump-light source for the excitation of photoacoustic waves. The third harmonic (355 nm) of a Nd:YAG laser pumps an optical parametric oscillator (OPO) that covers the wavelength range from 406 to 2500 nm. The

laser light is, if necessary, attenuated and focused into the sample. A pyro-electric detector at the back of the sample measures the energy of the transmitted laser pulses. The photoacoustic signal obtained gives still a relative value for the absorption coefficient and requires therefore a calibration.

### 3.2. Calibration

The PAS setup covers the wavelength range from 406 to 2500 nm. If there is an absorption band present in this range that can be measured with both, a standard grating spectrometer and the PAS, then a comparison of the data provides the calibration coefficient  $K$ . For a detailed description see [3]. In the available spectral range,  $\text{LiNbO}_3$  crystals exhibit only the band-edge absorption (Urbach tail) as an absorption feature that might be useful for this calibration. However, the linear absorption coefficient for wavelengths close to the band edge are difficult to measure with PAS due to the strong contribution of two-photon-absorption at typical intensities of the ns-laser pulses.

Thus, in the case of  $\text{LiNbO}_3$  crystals, the measurement has to be calibrated indirectly:  $\text{LiNbO}_3$  crystals contain hydrogen atoms bound as  $\text{OH}^-$  groups. A fundamental vibration of the  $\text{OH}^-$  group exhibits a strong absorption band around 2870 nm [11], which can be detected easily with standard grating spectrometers (see Fig. 1). The excitation of the first overtone of the  $\text{OH}^-$  vibration leads to an absorption band at 1470 nm. The ratio of the band intensities between fundamental and overtone excitations was determined by Förster et al. in proton exchanged lithium niobate to a value of 175 [12]. In undoped  $\text{LiNbO}_3$  the absorption band of the overtone is difficult to measure with standard transmission spectrometers, but can be observed with the PAS. Consequently, the PAS spectrum can be calibrated with the absorption band at 1470 nm, since its band intensity can be determined by measuring the fundamental  $\text{OH}^-$  absorption at 2870 nm with a standard spectrometer.

### 3.3. Results and limitations

Figure 3 shows the absorption spectra measured by the photoacoustic spectrometer for the undoped  $\text{LiNbO}_3$  sample. The  $\text{OH}^-$  overtone at 1470 nm used for the calibration is very pronounced for ordinarily polarized light.

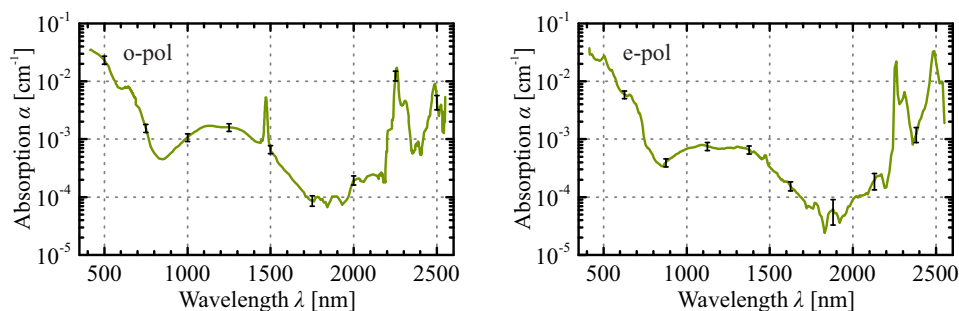


Fig. 3. Absorption spectra of undoped, congruently grown  $\text{LiNbO}_3$  for ordinarily (left) and extraordinarily (right) polarized light, measured with photoacoustic spectroscopy (PAS). See [Data File 1](#) and [Data File 2](#) for underlying values.

The absorption measurements with PAS are limited by the pump power available. In order to detect an absorption coefficient of  $10^{-5} \text{ cm}^{-1}$ , a pulse energy of 80 mJ would be needed (see Eq. (1) and [3]). Especially at the edge around 2500 nm the pulse energy of the OPO decreases significantly, leading to a higher inaccuracy of the measured values, as it can be

seen by the size of the error bars in Fig. 3. In the most transparent wavelength regime of the crystal at around 1750 nm, the detection limit of the method is reached, which corresponds to an absorption coefficient of about  $10^{-4} \text{ cm}^{-1}$ , as the maximal pulse energy here reaches only a few mJ. However, in materials with higher thermal expansion coefficients this value can be significantly lower [3].

Another limitation is the two-photon absorption, which plays a key role at the band edge, and prevents reliable measurements at wavelengths below 400 nm. In order to distinguish between single and two-photon absorption, the pump power can be varied. The PAS signal increases linearly with increasing pump power in the case of single photon absorption while it increases quadratically for two-photon absorption.

A systematic error can be caused by the calibration. For materials without an absorption feature within the covered wavelength window, a calibration is more sophisticated and thus only a relative value for the absorption is obtained.

#### 4. Photothermal common-path interferometry (PCI)

##### 4.1. Measurement principle

Photothermal common-path interferometry (PCI) is based on a phase-sensitive pump-probe technique [4]. A schematic of the setup is shown in Fig. 4. A strong continuous wave (cw) pump beam is focused into the sample and heats it locally due to light absorption. The rise in temperature leads to a local change of the refractive index and the center of the 2-4 times larger, weak probe beam, coinciding with the pump beam, undergoes a phase shift. During further propagation of the probe beam, the disturbed inner part of it interferes with the undisturbed outer part of the probe beam. A photodiode behind a pinhole detects the resulting intensity change in the center of the beam. To gain a higher sensitivity, the pump beam is modulated by a chopper wheel, and a lock-in amplifier is employed.

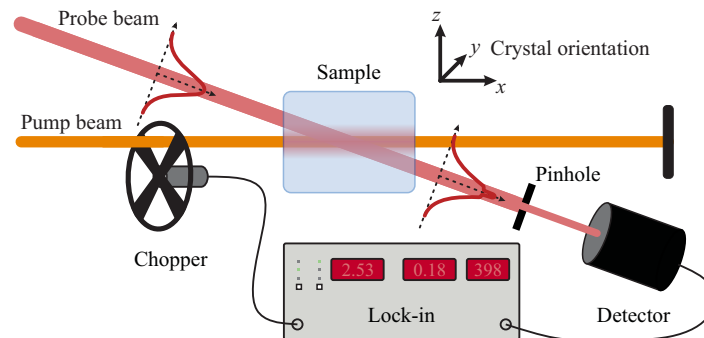


Fig. 4. Measurement principle of the photothermal common-path interferometer: The refractive index change caused by the absorbed energy of the pump beam leads to self interference of the probe beam. The intensity change in the probe beam center is detected by a photodiode. A Lock-In amplifier is used.

In the setup we employ as the pump source a self-built cw optical-parametric oscillator (OPO) with a power between 0.3 and 3 W. This OPO spans the wavelength regime from 1460 to 1880 nm for the signal wave and 2460 to 3800 nm for the idler wave. In order to achieve a better signal-to-noise ratio, the probe laser, a Helium-Neon laser, is power stabilized. The crossing angle of  $7^\circ$  between pump and probe laser gives a moderate resolution in the longitudinal direction of 0.5 to 1 mm, which enables to differentiate between bulk and surface absorption. The

LiNbO<sub>3</sub> sample has been mounted in the setup with the  $x$ -axis of the crystal in the pump beam direction and the  $z$ -axis in the pump-probe crossing plane (see Fig. 4). The chopper modulates the pump beam with 386 Hz.

#### 4.2. Calibration

The measured PCI signal is proportional to the absorption coefficient and to the pump power. The proportionality factor depends on setup parameters (beam sizes, crossing angle, probe beam polarization etc.) and material properties (thermo-optic and elasto-optic coefficients, thermal conductivity, thermal expansion, etc.). The easiest way for a calibration is like for the PAS the comparison of the PCI signal obtained in a strong absorption band to the measurement data of a standard spectrometer such as a GS or FTIR. If the material of interest does not show such a strong absorption band in the wavelength range available, one can also calibrate the setup itself. This is done by measuring the PCI signal for a highly absorptive sample (in our case NG 12 Schott Glass) with a known absorption coefficient and relating it to the absorption coefficient, obtained with one of the standard methods (GS or FTIR).

After this calibration, when studying other materials, the different properties are taken into account using a material correction factor. Once, this factor has been obtained for one setup and material, it can be applied to all comparable PCI setups, by using the setup correction factor. This calibration is independent of the polarization of the pump beam. Only the polarization of the probe beam has to be known. In the case of LiNbO<sub>3</sub> the material correction factor has been determined by Alexandrovski employing the absorption of a strongly iron-doped sample at 1064 nm with the  $z$ -axis of the crystal lying in the plane of the two crossing beams. To our knowledge this value (0.7, [5]) has not been published so far.

Having a widely tunable OPO as a pump source we could verify this factor for undoped LiNbO<sub>3</sub>, measuring the absorption coefficient in the fundamental OH<sup>-</sup> absorption band with its center at 2870 nm, thus, applying both methods for calibration. Since the absorption coefficient is well above 0.1 cm<sup>-1</sup> it can be measured by an FTIR. Figure 5 shows this comparison. The factor holds under the condition, that in addition to the  $z$ -axis also the  $x$ -axis of the crystal has to lie in the plane of the two crossing beams.

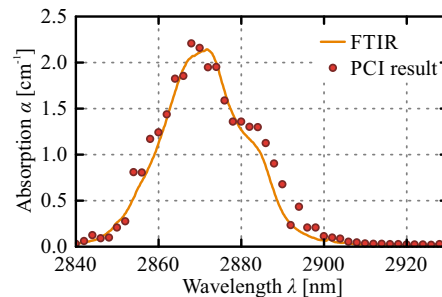


Fig. 5. FTIR measurement of the absorption coefficient of the fundamental OH<sup>-</sup> vibration band in LiNbO<sub>3</sub> at 2870 nm for ordinarily polarized light. The red circles are the calibrated PCI values, and the orange curve is the FTIR measurement of the sample.

#### 4.3. Results and limitations

The absorption spectra obtained with the PCI are shown in Fig. 6. The fundamental OH<sup>-</sup> vibration band at 2870 nm and its overtone at 1470 nm can be identified in the spectra. Both absorption bands are much weaker for extraordinarily than for ordinarily polarized light.

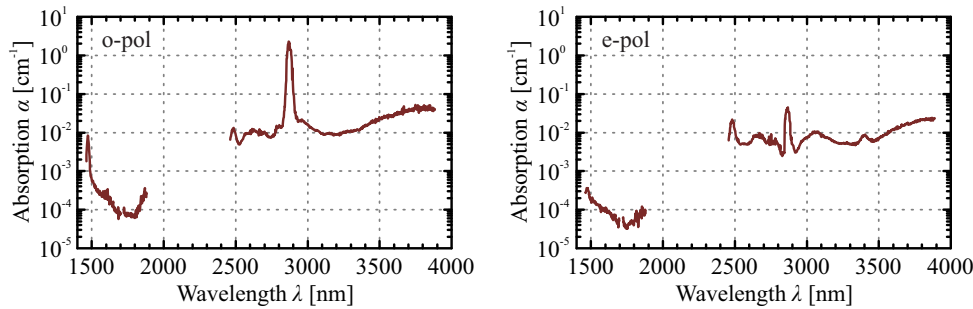


Fig. 6. The absorption spectra of undoped, congruently grown LiNbO<sub>3</sub> for ordinarily (left) and extraordinarily (right) polarized light, measured with photothermal common-path interferometry (PCI). See [Data File 3](#) and [Data File 4](#) for underlying values.

The detection limit of PCI depends mainly on the pump power available and the above mentioned properties of the investigated material. For the investigation of LiNbO<sub>3</sub> it is in our case  $10^{-5} \text{ cm}^{-1}$  for 1 W pump power. In the signal wavelength range from 1460 to 1880 nm the cw-OPO delivers typically more than 1 W, so the detection limit is below  $10^{-5} \text{ cm}^{-1}$ , which is one order of magnitude smaller than the values measured.

For very high light intensities a limitation of the technique is caused by nonlinear effects in the material such as the optical Kerr effect and two-photon absorption, which contribute to the change of the refractive index. For LiNbO<sub>3</sub>  $n_2$  is in the range of  $10^{-15} \text{ cm}^2/\text{W}$  [6]. Given the beam diameter of the pump beam in our setup (50 - 100  $\mu\text{m}$ ), these effects cause at a pump power around 100 W a refractive index change of  $10^{-9}$ , which corresponds to the detection limit of  $10^{-5} \text{ cm}^{-1}$  in the absorption coefficient. As pump powers of only a few Watt were used in the presented experiment, the nonlinear effects are negligible.

The error of the PCI signal after removing and again mounting the sample is below 5 %. In addition, the calibration may cause a systematic error. As described in the preceding chapter, the calibration delivers consistent results at strong absorption bands. However, it is difficult to evaluate, if the absorption coefficient cannot be measured by a standard spectrometer. Here doping of the material, as done by Alexandrovski for LiNbO<sub>3</sub>, can help.

## 5. Whispering-gallery-resonator-based absorption spectroscopy (WGRAS)

### 5.1. Measurement technique

In whispering gallery resonators (WGR) light is guided by total internal reflection. Quality factors, i.e. the number of oscillations required for the electric field to decay to  $e^{-\pi}$  of its initial value, of  $10^8$  lead to an effective optical path length of  $L_{\text{eff}} = Q\lambda/n \approx 50 \text{ m}$  in the material, where  $\lambda \approx 1 \mu\text{m}$  is the wavelength and  $n \approx 2$  the refractive index of the resonator. Thus, the sensitivity of absorption measurements should be orders of magnitude higher for WGRAS than for GS or FTIR.

We position a prism of higher refractive index than that of the resonator close to the WGR employing evanescent wave coupling. In order to match the modes of the resonator, the laser source frequency is tuned without mode hops. As laser sources we use a tunable Ti:sapphire laser without and with frequency doubling as well as an OPO pumped by the Ti:sapphire laser. Thus, the wavelength regions from 700 to 1000 nm (Ti:sapphire laser), from 350 to 500 nm (frequency doubled Ti:sapphire laser), from 1000 to 1500 nm for the signal wave and from 1700 to 2600 nm for the idler wave of the OPO are covered. In combination, a large part of

the transparent region of the material is covered. The distance  $d$  between prism and resonator can be varied by a piezo actuator (see Fig. 7 (left)). A detector is positioned at the back of the prism to measure the power of the light reflected by the prism base. By monitoring the pump light versus the frequency shift of the laser one can measure the linewidth of the respective resonator modes (see Fig. 7 (right)). From the linewidth  $\Delta\nu_{\text{FWHM}}$  the  $Q$ -factor can be calculated by  $Q = \nu_0/\Delta\nu_{\text{FWHM}}$ , where  $\nu_0$  is the center frequency of the pump light.

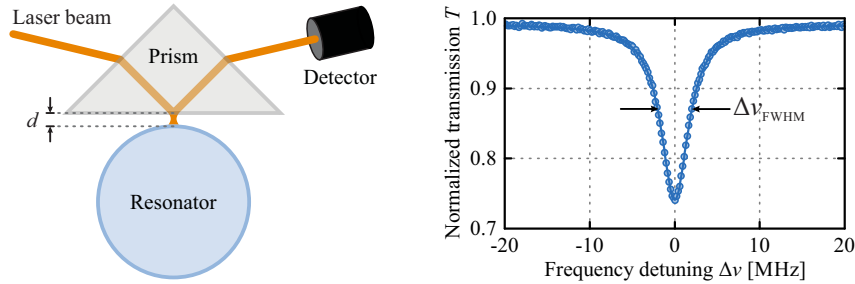


Fig. 7. Left: Experimental setup. Right: WGR mode. From its linewidth, the  $Q$ -factor can be calculated.

The  $Q$ -factor of the resonator results mainly from three loss mechanisms: coupling loss, surface scattering, and bulk loss including bulk absorption and bulk scattering:

$$\frac{1}{Q} = \frac{1}{Q_c} + \frac{1}{Q_\sigma} + \frac{1}{Q_\kappa}. \quad (2)$$

Here  $Q_c$ ,  $Q_\sigma$  and  $Q_\kappa$  quantify these loss mechanisms.

The coupling loss decreases exponentially with  $d$  [13]. Thus,  $Q_c^{-1}$  can be neglected in Eq. (2). In order to be able to neglect surface scattering, the WGR is polished with a diamond slurry. Atomic force microscope (AFM) measurements of the surface of the resonator show that the surface roughness is sufficiently small to neglect  $Q_\sigma^{-1}$  in Eq. (2). Thus,  $Q$  is given solely by the bulk losses from which the extinction coefficient can be calculated by using  $Q_\kappa = 2\pi n/(\kappa\lambda)$  [8]. Thus, by measuring the intrinsic linewidth  $\Delta\nu_{\text{intr}}$  for large distances  $d$ , one can calculate an absolute value for the extinction coefficient  $\kappa$  of the material.

## 5.2. Results and limitations

The results of the extinction measurements obtained by WGRAS are shown in Fig. 8 for o- (left) and e-polarized light (right). The onset of the band edge ( $\kappa \approx 10^{-2} \text{ cm}^{-1}$ ) can be resolved as well as the most transparent regime ( $\kappa = 9 \times 10^{-5} \text{ cm}^{-1}$ ) of  $\text{LiNbO}_3$  at around 1750 nm. Furthermore, for o-polarized light the overtone of the  $\text{OH}^-$  vibration band at 1470 nm, is clearly seen.

A limit of this technique is given by the linewidth of the scanning laser – in our case being around 100 kHz. It has to be lower than the linewidth of the measured resonator mode to be able to resolve the latter. The results shown in this work extend to the edge of the measurable extinction coefficient of around  $5 \times 10^{-5}$ . To overcome this limit, one can perform cavity ring-down measurements with the WGR [14].

Uncertainties using WGRAS arise from the fits to the data to get  $\Delta\nu_{\text{FWHM}}$  and  $Q_{\text{intr}}$  (below 10 %). Furthermore, WGR modes in the observed spectrum may overlap, resulting in an over-estimated linewidth. Therefore, in general all points shown in Fig. 8 represent an upper limit for the extinction. In contrast to the other two techniques presented, WGRAS does not require a calibration to measure the extinction coefficient, which reduces the systematic error of the

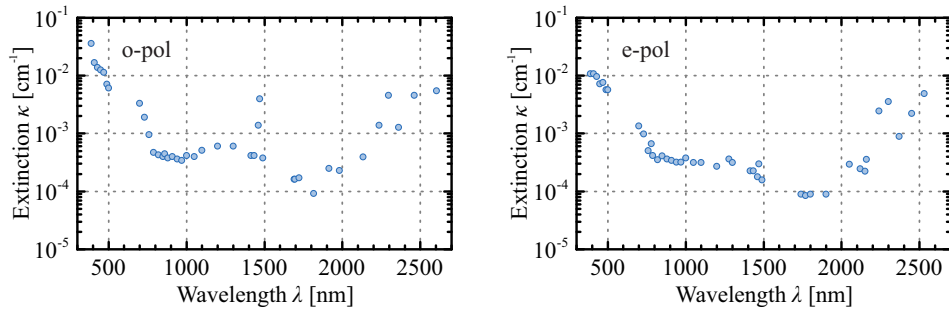


Fig. 8. Extinction coefficient of undoped, congruently grown  $\text{LiNbO}_3$  for ordinarily (left) and extraordinarily (right) polarized light, measured by whispering-gallery-resonator-based absorption spectroscopy (WGRAS). See [Data File 5](#) and [Data File 6](#) for underlying values.

measurement.

## 6. Absorption spectra: comparison and discussion

The absorption spectra of undoped, congruently grown lithium niobate ( $\text{LiNbO}_3$ ) measured with the three described techniques are shown in Fig. 9(a) and 9(b) for comparison. For a better clarity they are divided in measurements with ordinarily (see Fig. 9(a)) and extraordinarily (see Fig. 9(b)) polarized light. Together, the methods cover the wavelength range from 390 to 3800 nm, which includes the window of highest transparency of the crystal. The absorption coefficient is measured from below  $10^{-4} \text{ cm}^{-1}$  at around 1750 nm up to  $2 \text{ cm}^{-1}$  at the fundamental  $\text{OH}^-$  absorption at 2870 nm. The measurements performed with PAS and PCI have been calibrated independently.

The absorption starts at 390 nm in the range of  $10^{-2} \text{ cm}^{-1}$  and drops with increasing wavelength for both polarizations. This absorption in the visible spectral range can be referred to  $\text{Fe}^{2+}$  impurities in the crystal [15]. Such impurities originate usually from impurities in the crucibles that are used for the growing process. At around 820 nm the absorption reaches a local minimum with a value of around  $4 \times 10^{-4} \text{ cm}^{-1}$  before an absorption band between 1000 and 1500 nm rises, which is stronger for o- than for e-polarized light. This absorption band can also be attributed to  $\text{Fe}^{2+}$  impurities [15].

The overtone at 1470 nm of a known  $\text{OH}^-$  absorption band, centered at 2870 nm [9] is observable with all three techniques. As expected, it is stronger for o-polarized light. Towards higher wavelengths, the value drops to its minimum of around  $10^{-4} \text{ cm}^{-1}$  between 1700 and 1800 nm, before rising again. The maxima at 2260 and 2480 nm wavelengths, which have already been observed in FTIR measurements of magnesium-doped  $\text{LiNbO}_3$  by Vainio et al. [16], are seen clearly. They result from mixed  $\text{OH}^-$  stretching and libration transitions. The absorption coefficient around the latter maximum is higher for e-polarized light. The already mentioned  $\text{OH}^-$  absorption at 2870 nm is clearly visible for both polarizations, while it is stronger for o-polarized light. The following maxima for e-polarized light at 3100 and 3400 nm have also been observed by Vainio et al. in magnesium-doped lithium niobate, with the first one frequency shifted to below 3000 nm. At around 3300 nm the multiphonon absorption band starts to dominate the measurements and its contribution increases with longer wavelengths.

In general the measurements coincide very well, although for WGRAS the extinction coefficient is shown. Furthermore, for WGRAS there is no  $\lambda^{-4}$ -dependence for the extinction coefficient observable, what is the typical dependence for Rayleigh scattering, the main contribution to bulk scattering. Both facts lead to the conclusion that absorption is the dominating

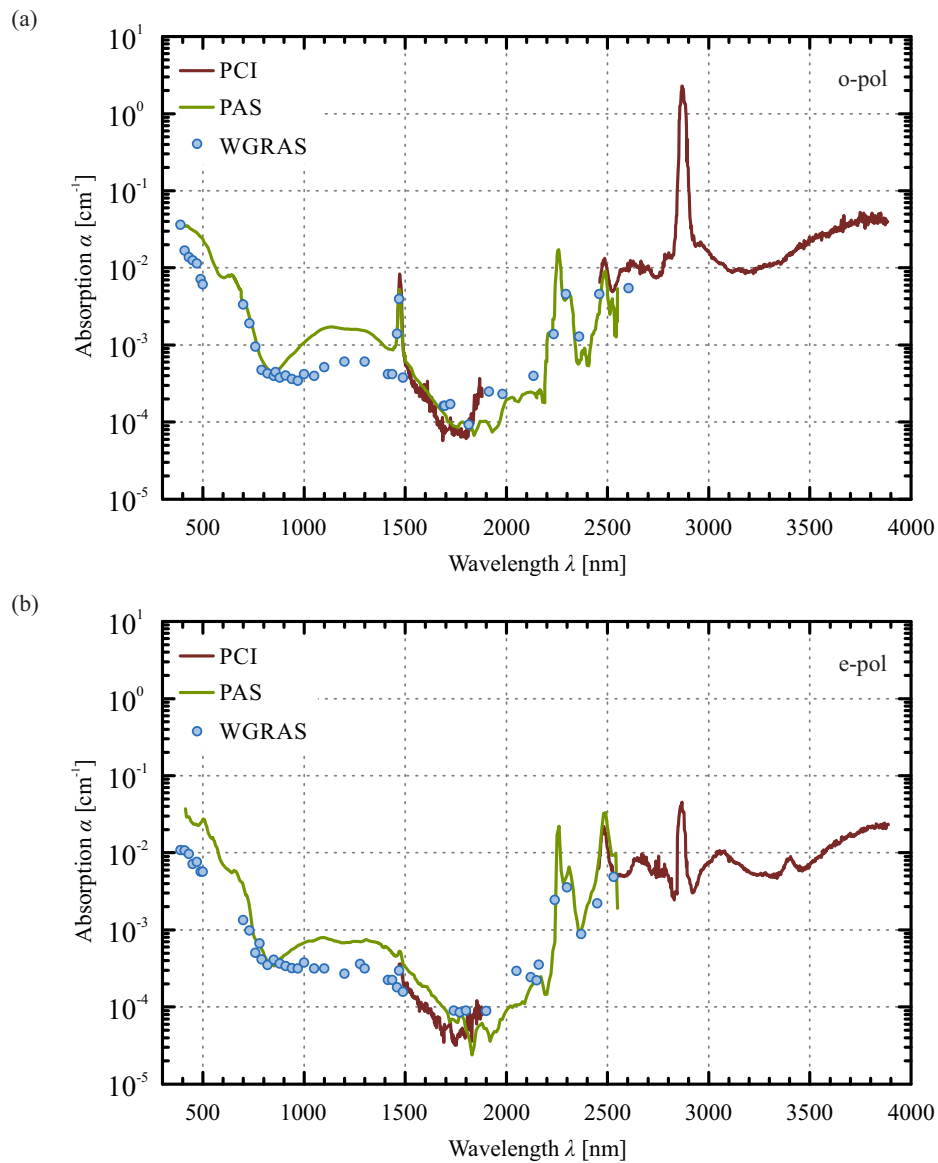


Fig. 9. Absorption spectra of undoped, congruently grown LiNbO<sub>3</sub> in logarithmic scale (a) for ordinarily and (b) for extraordinarily polarized light: The results from the measurement of a photoacoustic spectrometer (PAS), a photothermal common-path interferometer (PCI) and a whispering-gallery-resonator-based absorption spectrometer (WGRAS) are shown.

contribution to the extinction in LiNbO<sub>3</sub> and not bulk scattering. So the labeling in Fig. 9, stating the Lambert-Beer coefficients  $\alpha$ , is valid. Another consequence of the equality of the absolute values is, that the different calibrations for PAS and PCI hold, even for absorption coefficients of the order of  $10^{-3}$  to  $10^{-4}$  cm<sup>-1</sup>.

However, there are some differences in the spectra shown. In the blue and green region and in the band from 1000 to 1500 nm, PAS leads to a higher absorption coefficient than WGRAS. These differences may originate from multiple-photon processes in the material. These effects can be seen only for PAS because it utilizes a pulsed light source in contrast to WGRAS, where weak CW light is used. For the blue and green region, two-photon absorption is most likely the additional loss mechanism, as starting from 600 nm, towards the band edge, the cross-section for two-photon absorption is non-zero and increasing. For the absorption band around 1100 nm a three photon absorption process could explain the difference [17]. One IR photon excites Fe<sup>2+</sup> impurity ions into a crystal-field splitting level, and from this excited state a two-photon absorption process transfers the electrons into the conduction band. We conclude that the results for WGRAS are more trustworthy in these wavelength regions than the ones obtained by PAS.

In the absorption minimum around 1750 nm all methods show similar values although, especially for e-polarized light, the results begin to differ. Considering the fact, that all techniques get here close to their detection limit and thereby the uncertainties get larger, the spreading of a factor two for the measured values is still a good agreement.

From the successful calibration of the PAS measurement it can be concluded that the ratio of the band intensities of fundamental and overtone OH<sup>-</sup> vibrations has indeed in undoped lithium niobate a value of about 175. This number was originally taken from studies with proton exchanged lithium niobate by Förster et al. [12].

Savchenkov et al. published an estimation for the *Q*-factor of different WGRs made of LiNbO<sub>3</sub> of different compositions without specifying the polarization [8]. The estimation consists in a model for the absorption coefficient only considering the losses caused by UV absorption, bulk Rayleigh scattering and multiphonon absorption:

$$\alpha \simeq \alpha_{\text{UV}} e^{\lambda_{\text{UV}}/\lambda} + \alpha_{\text{R}} \lambda^{-4} + \alpha_{\text{IR}} e^{-\lambda_{\text{IR}}/\lambda} \quad (3)$$

Here,  $\alpha_{\text{UV}}$ ,  $\lambda_{\text{UV}}$ ,  $\alpha_{\text{R}}$ ,  $\alpha_{\text{IR}}$  and  $\lambda_{\text{IR}}$  are the parameters determining the above mentioned absorption types. The extrapolation based on the semiphenomenological model Eq. (3) and the by Savchenkov et al. collected fragmentary data on absorption is shown in Fig. 10 (left). Due to the lack of data, the fit is limited to a rather small wavelength region. In this region he gives a projected lower absorption limit for LiNbO<sub>3</sub> of  $10^{-4}$  cm<sup>-1</sup>. A fit to our more integral data using the same model Eq. (3) is shown in Fig. 10 (right). It gives a theoretical absorption minimum of  $10^{-5}$  cm<sup>-1</sup>, so an order of magnitude lower than the estimation given by Savchenkov et al. In principal the model describes the absorption quite good although not as good as, e.g., in the case of optical fibers, where the theoretical limit described with the model given by Eq. (3) for the absorption coefficient can be reached [18]. From the fit made based on our data it is obvious that for a more accurate description the model has to be expanded by the absorption caused by the above mentioned impurities. Nevertheless, the theoretical limit seems to be reachable by removing these impurities.

Now we compare the data achieved with that from standard GS, which is possible only in the regions where the absorption exceeds  $10^{-2}$  cm<sup>-1</sup>, i.e. between 350 and 800 nm, and between 2200 and 3000 nm. results are shown in Fig. 11(a) for the visible wavelength range and in Fig. 11(b) for the NIR regime. In the visible spectral range, WGRAS and the GS show accurate agreement, while the PAS values are higher, which has been explained above. In the infrared regime the PAS, PCI and GS data show good agreement for both polarizations in the absorption bands at 2260, 2480 and at 2870 nm. Slight differences of the absolute values of these peaks

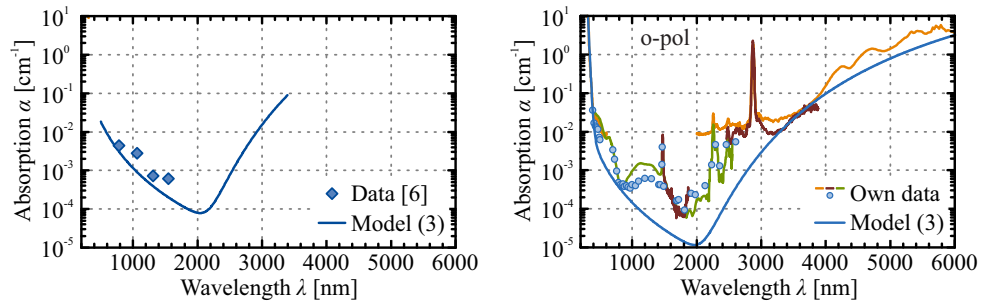


Fig. 10. Left: Data for the absorption coefficient of  $\text{LiNbO}_3$  collected by Savchenkov et al. (blue dots, polarization of the light not given) together with his estimation for the theoretical shape of the absorption. Right: Absorption coefficient measured by PAS, PCI and WGRAS of undoped, congruently grown  $\text{LiNbO}_3$  for ordinarily polarized light with the fit using the same model.

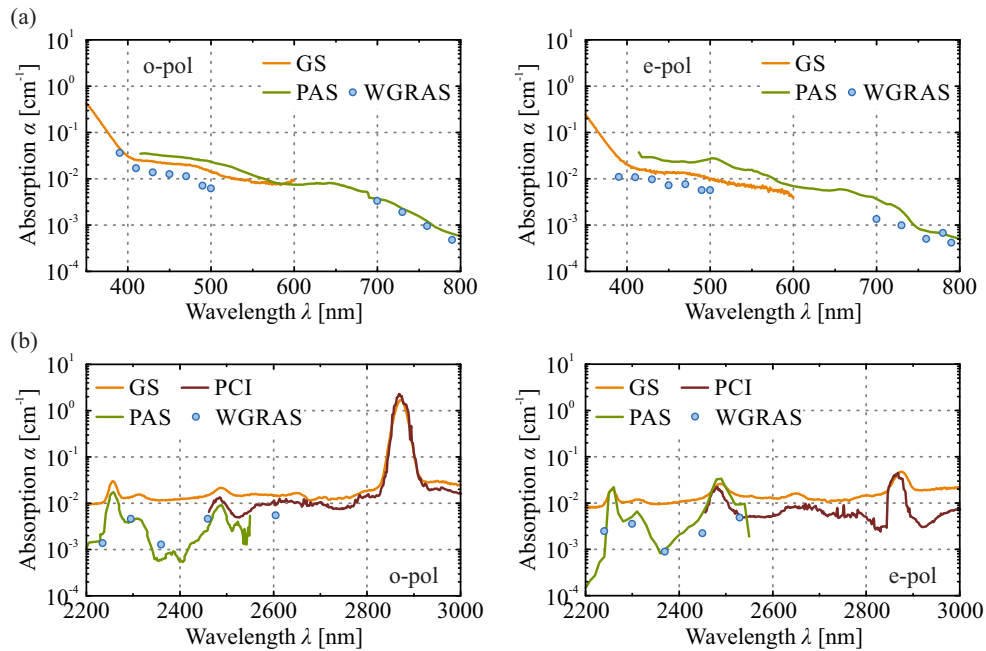


Fig. 11. Comparison of the absorption coefficient measured by PAS, PCI and WGRAS of undoped, congruently grown  $\text{LiNbO}_3$  with values obtained by studying the same sample with a standard GS in (a) the visible and (b) the near infrared light range. Left: ordinarily polarized light. Right: extraordinarily polarized light.

and at absorption values below  $10^{-2} \text{ cm}^{-1}$  are due to the fact, that the detection limit of the GS of about 1 % per 1 cm sample length is reached. Together, this comparison shows, that all three methods are reliable to measure low absorption.

## 7. Comparison of the applied methods

Generally, a difference between PAS and PCI on the one hand and WGRAS on the other hand is, that latter one measures the extinction coefficient, while first ones measure the absorption. If the extinction is dominated by absorption, like in the investigated case, they coincide. For some applications, like studies of the damage threshold of a material, only the absorption is of relevance. If such materials exhibit simultaneously scattering and absorption, then WGRAS is not a good choice.

The main disadvantage for PAS and PCI is the calibration. Both require a strong absorption band being present in the measurable wavelength range. Otherwise one obtains only a relative picture of the absorption. WGRAS measures in contrast an absolute value. But it is a destructive method, because a resonator has to be manufactured out of the material of interest. Also the manufacturing process of the resonator requires several steps and the polishing has to be good enough in order to neglect surface scattering. However, for PAS and PCI, the samples have to be polished just to optical quality and have to fit into the setup - but they have to be larger than those for WGRAS.

Regarding the availability of laser sources, PAS has a big advantage, as it uses a pulsed source. This laser type is commercially available for a broad range of wavelengths. For cw light this is not yet the case, especially not with the power, that PCI requires. WGRAS only requires a light power of some  $\mu\text{W}$ , which makes the search for a suitable light source easier, but mode-hop-free tuning and a narrow linewidth are needed.

The sensitivities for PAS, PCI and WGRAS are for  $\text{LiNbO}_3$  quite the same. For PAS and PCI it increases with increasing light power. This means that for a high sensitivity, high power is needed which may lead to non-desired effects, affecting the absorption measurements. For PAS, as shown, nonlinear absorption, such as multiple-photon processes and for PCI the non-linear Kerr effect can play a role. For the weak powers as they are used for WGRAS such problems do not exist. Here, the sensitivity can be enhanced by cavity ring-down measurements and thereby solely is limited by the polishing of the resonator surface. The highest yet published  $Q$ -factor of  $10^{11}$  for  $\text{CaF}_2$  [19] results in an extinction coefficient of  $6 \times 10^{-7} \text{ cm}^{-1}$ .

Considering the speed of data acquisition, PAS and PCI show strong advantages as they can be totally automated. The time needed to obtain a spectrum is still quite large for WGRAS, as the alignment of the evanescent field coupling has to be done so far for all individual wavelengths.

In conclusion, a combination of PAS or PCI with WGRAS could be the most advanced way to measure low absorption. The absolute value can be measured with WGRAS at some wavelengths, and this value can then be used for the calibration of the other, faster methods. For the region of higher absorption, standard methods like GS or FTIR can be employed. Combining all the methods, a material can be fully characterized regarding its absorption coefficient. In this study, this is done for the first time for undoped, congruently grown  $\text{LiNbO}_3$ . Its absorption coefficient for the whole transparency window from around 380 to 6000 nm is shown in Fig. 12 for o- and e-polarized light.

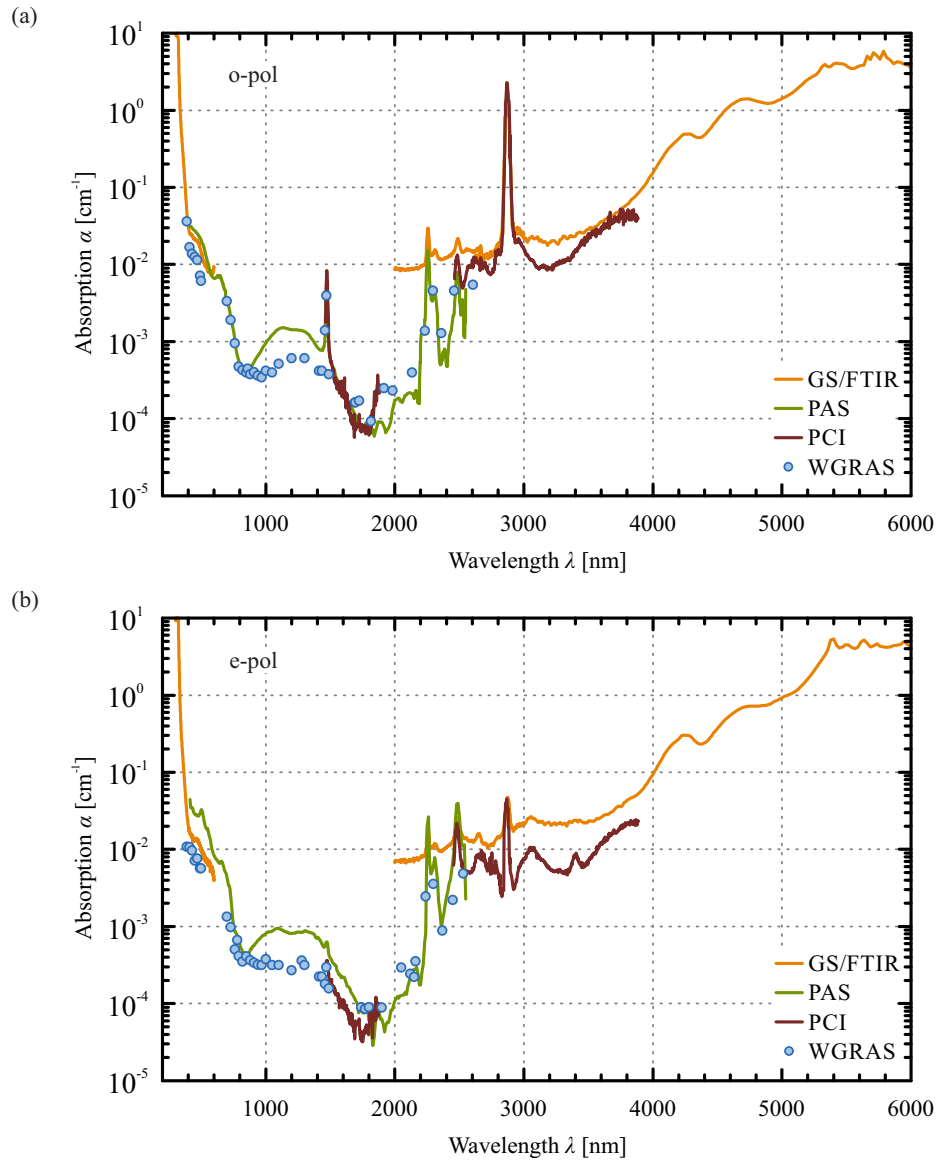


Fig. 12. Absorption spectra of congruently grown  $\text{LiNbO}_3$  for the entire transparency window, measured by PAS, PCI, WGRAS, GS and FTIR. (a): ordinarily polarized light. (b): extraordinarily polarized light.

## 8. Conclusion

For the first time, we have measured the absorption coefficient of an undoped, congruently grown lithium niobate crystal in its entire transparency window from 320 to 6000 nm for ordinarily and extraordinarily polarized light using three independent, highly sensitive spectroscopy techniques (PAS, PCI and WGRAS), as well as two standard spectrometer types (GS, FTIR). The absorption coefficient varies over more than five orders of magnitude. The minimum value measured for the absorption is about  $10^{-4} \text{ cm}^{-1}$  at 1750 nm wavelength.

The comparison of the results obtained by different methods shows good agreement. This punctuates the reliability of the techniques and, in the case of PAS and PCI, their calibration.

## Acknowledgment

Financial support from Deutsche Forschungsgemeinschaft and Fraunhofer-Gesellschaft (Attract grant 692247) is gratefully acknowledged.